JOURNAL OF GEOPHYSICAL RESEARCH: SPACE PHYSICS, VOL. 118, 785–793, doi:10.1002/jgra.50091, 2013

Ion temperature anisotropy instabilities in planetary magnetosheaths

B. Remya,[1] R. V. Reddy,[1] B. T. Tsurutani,[2] G. S. Lakhina,[1] and E. Echer[3]

Received 2 October 2012; revised 7 December 2012; accepted 18 December 2012; published 28 February 2013.

[1] There has been a lack of understanding why mirror modes are present in planetary magnetosheaths, at comets, and in the heliosheath. Linear theory indicates that the ion cyclotron instability should dominate over the mirror mode instability in electron-proton plasma. In this paper, we take a new approach. We examine the role of plasma electron temperature anisotropy on the ion cyclotron and mirror mode instabilities. It will be shown that an inclusion of anisotropic electrons with $T_{\perp e}/T_{\| e} \geq 1.2$ reduces the ion cyclotron growth rate substantially and increases the mirror mode growth rate. The minimum plasma beta for mirror instability dominance (over the ion cyclotron instability) is $\beta_p = 0.5$.

Citation: Remya, B., R. V. Reddy, B. T. Tsurutani, G. S. Lakhina, and E. Echer (2013), Ion temperature anisotropy instabilities in planetary magnetosheaths, *J. Geophys. Res. Space Physics*, *118*, 785–793, doi:10.1002/jgra.50091.

1. Introduction

[2] Certain locations of the Earth's magnetosheath have been observed to have anisotropic ion distributions with its perpendicular temperature greater than the parallel temperature, $T_{\perp i} > T_{\| i}$, where $T_{\perp i}$ and $T_{\| i}$ indicates the ion perpendicular and parallel temperatures relative to the background magnetic field B_0, respectively. These anisotropic distributions, caused by heating at the quasi-perpendicular bow shock and magnetic field draping around the magnetosheath, act as the source of free energy to drive various low frequency instabilities in the magnetosheath [*Midgley and Jr. Davis*, 1963; *Zwan and Wolf*, 1976; *Gary et al*., 1976; *Lee et al*., 1988]. Among them the two major electromagnetic instabilities that compete with each other are the mirror instability and the electromagnetic ion cyclotron anisotropy instability (hereafter referred to as MI and ICI, respectively). The competition between these two instabilities has been a topic of study for the past few decades [*Winske and Quest*, 1988; *Gary*, 1992; *Gary et al*., 1993a, 1993b; *Anderson and Fuselier*, 1993; *Schwartz et al*., 1996; *Shoji et al*., 2009; 2012].

[3] The mirror instability is characterized by a zero real frequency in the plasma frame. Mirror modes are quasi-periodic structures with typical mean scale sizes of about $20\rho_p$ in the Earth's magnetosheath [*Tsurutani et al*., 1982; *Lucek et al*., 2001], 20–$40\rho_p$ in the Jovian and Saturnian magnetosheaths [*Tsurutani et al*., 1982; *Erdös and Balogh*, 1996] and about 80 to a few hundreds of ρ_p in the heliosheath [*Burlaga et al*., 2006; 2007; *Tsurutani et al*., 2010]. In the above, ρ_p is the proton gyro radius. The structures are characterized by plasma densities being anticorrelated with magnetic pressure, where total pressure remains constant. Mirror modes have a maximum growth rate at wave vector directions oblique to the background magnetic field and hence have a substantial longitudinal magnetic field component. From fluid theory, the criterion for the excitation of mirror instability by anisotropic ions is $\beta_\perp/\beta_\| > 1 + 1/\beta_\perp$ [*Chandrasekhar et al*., 1958; *Vedenov and Sagdeev*, 1958; *Barnes*, 1966; *Hasegawa*, 1969], where β is the ratio of plasma kinetic to magnetic pressure. The ion cyclotron anisotropy instability is characterized by a non-zero real frequency with maximum growth rate parallel to the background magnetic field. The waves are observed at frequencies less than or equal to proton cyclotron frequency. The ion cyclotron instability is a resonant instability with resonant ions and non-resonant electrons and is well explained by a kinetic approach [*Kennel and Petschek*, 1966]. While mirror modes are likely to be prevalent in the high beta regions of the magnetosheath proper [*Tsurutani et al*., 1982; *Song et al*., 1992; *Anderson and Fuselier*, 1993], the ion cyclotron modes are strongly observed under low beta plasma conditions [*Sckopke et al*., 1990; *Anderson and Fuselier*, 1993].

[4] There are a number of observations of mirror mode structures in the Earth's magnetosheath [*Kaufmann et al*., 1970; *Tsurutani et al*., 1982; 1984]. Apart from that, there are various other space plasma regions like the solar wind [*Tsurutani et al*., 1992], cometary magnetospheres [*Russell et al*., 1987; *Tsurutani et al*., 1999], magnetosheath of other planets like Jupiter and Saturn [*Tsurutani et al*., 1982; *Erdös and Balogh*, 1996], and in the heliosheath [*Burlaga et al*., 2006; *Tsurutani et al*., 2010; 2011] where mirror modes are found to grow. The ion temperature anisotropy $T_{\perp i} > T_{\| i}$ can also excite the left-hand polarized ion cyclotron anisotropy instability in the magnetosheath [*Kennel and Petschek*, 1966; *Sckopke et al*., 1990; *Lacombe et al*., 1992; *Tsurutani et al*., 2000]. Most of the theoretical and computational studies show that the ion cyclotron instability has a higher growth rate compared to the mirror instability for a given set of plasma parameters in electron-proton plasma. In sharp contrast, most of the observations in the magnetosheath show frequent

[1]Indian Institute of Geomagnetism, Navi Mumbai, India.
[2]Jet Propulsion Laboratory, California Institute of Technology, Pasadena, California, USA.
[3]Instituto Nacional de Pesquisas Espaciais (INPE), São Jose dos Campos, Brazil.

Corresponding author: B. Remya, Indian Institute of Geomagnetism, Kalamboli Highway, New Panvel, Navi Mumbai, Maharashtra, India. (remyaphysics@gmail.com)

2169-9380/13/10.1002/jgra.50091

occurrence of mirror instability rather than ion cyclotron instability. *Gary* [1992] numerically solved the complete electromagnetic dispersion relation to prove that the proton cyclotron instability has higher growth rate than the mirror instability for a wide range of parameters in an electron-proton plasma with $T_e = T_p$. *Price et al.* [1986] showed that the presence of helium ions in the plasma reduces the growth rate of the ion cyclotron instability significantly whereas the mirror growth rate remains almost unaltered. This may lead to a situation where the mirror instability can dominate the ion cyclotron instability in sufficiently high beta plasmas ($\beta_p \geq 4.0$) [*Gary*, 1992; *Gary et al.*, 1993]. *Shoji et al.* [2009; 2012], using two- and three-dimensional simulations, analyzed the two competing modes and suggested that the large volume of mirror waves in three-dimensional space consumes most of the free energy of the temperature anisotropy and thus stops the growth of the ion cyclotron waves. According to them, the mirror-mode structures have wave number vectors mostly in the oblique directions and thus their wave number spectra become like a "torus." At the same time, the nonlinear evolution of ion cyclotron waves undergo wave-particle interaction and loses energy.

[5] This paper is a pioneer study of electron anisotropy effects on the competition between mirror and ion cyclotron modes. The paper presents a parametric model of the planetary magnetosheaths covering a wide range of parameters. Earlier, *Lakhina and Buti* [1976] found that electron temperature anisotropy tends to suppress the ion cyclotron instability growth rate in solar wind double ion streams. Just like ions, electrons also get anisotropically heated to approximately the same values in the planetary magnetosheaths. Previous studies have treated electrons as isotropic due to the presumption that wave-particle interactions will isotropize the electrons faster than the ions. *Tsurutani et al.* [1982] and *Lee et al.* [1987] had used three-dimensional distribution function calculations from ISEE vector electron spectrometer data and a theoretical model, respectively, to study the electron dynamics of the lion roars (electron cyclotron waves) and mirror waves in the Earth's magnetosheath. *Tsurutani et al.* [1982] determined that the electron temperature anisotropy $T_{\perp e}/T_{\| e}$ is generally greater than 1.0, with the largest values (up to 1.2) occurring in the minimum field regions. *Lee et al.* [1987] suggested that the electron temperature anisotropy is higher in the low magnetic field region and vice versa. *Thomsen et al.* [1985] explain the heating of the electrons across collisionless shocks and suggest that although the electrons isotropize faster than the ions, there are times when electrons do exhibit a $T_{\perp e} > T_{\| e}$ anisotropy in the Earth's magnetosheath. Recently, *Masood and Schwartz* [2008] have used Cluster observations in the Earth's magnetosheath to show that the electrons exhibit significant temperature anisotropy $T_{\perp e} > T_{\| e}$ in the deep magnetosheath while being isotropic just behind the bow shock. The former effect is most likely due to magnetic field line draping. In this paper, the electron temperature anisotropy effects on the growth rates of the mirror and ion cyclotron instabilities are studied for the first time and it is determined that electron anisotropy plays a major role in determining which mode dominates in each plasma region. The plasma beta, temperature, anisotropy, and density parameters used for the numerical solutions are not based upon any specific observation but in general model the magnetosheath plasma properties based on various observations [*Anderson et al.*, 1991; *Fuselier et al.*, 1991; *Anderson and Fuselier*, 1993; *Soucek and Escoubet*, 2011].

[6] The aim of this study is to demarcate the parametric regimes over which the mirror and ion cyclotron instabilities are sustained and to provide an answer for the prominent mirror mode observations in the magnetosheath. The fully kinetic electromagnetic dispersion relation is solved numerically for a bi-Maxwellian particle distribution using the WHAMP (Waves in Homogeneous Anisotropic Multicomponent/Magnetized Plasma) [*Ronnmark*, 1982, 1983] code in a homogeneous multi-component plasma consisting of anisotropic electrons, protons, and minor ions $^4He^{2+}$ and $^{16}O^{6+}$. The code is used to solve the low-frequency electromagnetic kinetic dispersion relation for a varied range of ion temperature anisotropy and ion plasma β (β being the ratio of plasma kinetic pressure to magnetic pressure) at arbitrary wavelengths and arbitrary angles of propagation. Studies show that the parameters $\frac{T_{\perp i}}{T_{\| i}}$, β_i, the concentration of heavy ions, and the electron temperature anisotropy all play a crucial role in determining which instability dominates in each region. Section 2 in this paper demonstrates the magnetosheath plasma model and defines the parameters for our study. Section 3 gives a case-by-case study of each instability in specific parametric regimes. The discussion attempts to determine the factors that affect the growth rates of the mirror as well as the ion cyclotron instabilities and to define the parametric regimes over which each instability dominates. The paper concludes with a summary and conclusion section (sections 4 and 5, respectively).

2. The Magnetosheath Plasma Model

[7] The plasma model that we consider here is a homogeneous, unperturbed, charge neutral plasma in a uniform background magnetic field $\overrightarrow{B_0}$ directed along the $\hat{z}$ axis. The wave vector k is in the x-z plane, so that $\overrightarrow{k} = k_x\hat{x} + k_z\hat{z}$ and makes an angle θ with B_0. The waves are considered to be plane transverse waves with fluctuations varying in space and time as $\exp(ik_x x + ik_z z - i\omega t)$, where the wave vector components are taken to be real and the frequency ω is assumed to have a real and imaginary component $\omega = \omega_r + i\gamma$.

[8] Our study uses mainly two models. Our first model, a multi-species plasma, includes contributions from anisotropic heavy ions such as $^4He^{2+}$ and $^{16}O^{6+}$ along with anisotropic protons and isotropic electrons. The latter are included in the model to accurately simulate the solar wind. Heavy ions other than helium and oxygen have even lower or negligible concentrations and hence not considered in our study [*Bame et al.*, 1968, 1970]. Our second model contains anisotropic protons, anisotropic heavy ions $^4He^{2+}$ and $^{16}O^{6+}$, and anisotropic electrons. Measurements of He in the solar wind indicate that the densities are variable, ranging between 1 % and 10 %. Thus, our models consider variable helium concentrations of $n_\alpha = 0.01n_p$, $n_\alpha = 0.04n_p$, and $n_\alpha = 0.10n_p$ with isotropic electrons (model 1) and anisotropic electrons (model 2). The oxygen ion concentration is assumed to be about 4 % of the helium ion concentration. Various parameters for different species will be denoted with subscripts "e" for electrons, "p" for protons, "α" for $^4He^{2+}$, and "O" for $^{16}O^{6+}$, and ions in general with "i." The temperature anisotropy due to heating of the particles across the quasi-perpendicular bow shock or by draping of the magnetic field

lines is assumed to be equal for all the plasma species (except for electrons). Therefore, the temperature and anisotropy of all the ion species are assumed to be the same. The electrons dissipate their energy due to wave-particle interactions and scatter to isotropy faster as compared to the ions. Hence they are assumed to have anisotropies considerably less than that of protons. Plasma betas in the magnetosheath are assumed to vary from sufficiently low values ($\beta_p = 0.5$ or lesser) close to the magnetopause [*Anderson and Fuselier*, 1993] to higher betas ($\beta_p \geq 4.0$) [*Anderson et al*., 1991; *Anderson and Fuselier*, 1993] at the magnetosheath proper.

[9] All the components are assumed to have a bi-Maxwellian zeroth order distribution function given by

$$f_j^{(0)}(v_z, v_\perp) = \frac{n_j}{\left(\pi v_{thj}^2\right)^{3/2}} \frac{T_{\|j}}{T_{\perp \mathrm{j}}} \exp\left[-\frac{v_z^2}{v_{thj}^2} - \frac{v_\perp^2}{v_{thj}^2}\frac{T_{\|j}}{T_{\perp \mathrm{j}}}\right] \quad (1)$$

where j represents each species, velocity $\vec{v}_\perp = v_x\hat{x} + v_y\hat{y}$, and the subscripts $\|$ and $\perp$ indicate directions parallel and perpendicular to B_0, respectively. The thermal velocity is given as $v_{thj} = \sqrt{2k_B T_{\|j}/m_j}$ for each species j. The cyclotron frequency is given by $\Omega_j = \frac{q_j B_0}{m_j c}$ and the plasma beta $\beta_j = \frac{8\pi n k_B T_\|}{B_0^2}$, where c is the velocity of light in free space, n is the density of protons, and k_B is the Boltzmann constant. The anisotropy for each species will be denoted as $A_j = \frac{T_{\perp j}}{T_{\|j}}$. Zero relative drift is assumed among the components. The full linear electromagnetic dispersion equation is derived by considering the general theory of linear Vlasov waves for charge-neutral, homogeneous, collisionless plasma [*Stix*, 1962]. The derivation is based on the above described plasma and wave models.

3. Competition Between Mirror and Ion Cyclotron Anisotropy Instability

[10] What is(are) the factor(s) affecting the growth rates of the mirror and the ion cyclotron anisotropy instability in these parametric regions? We undertake a case-by-case parametric study as an effort to answer this question and show that the plasma parameters (β_p, $T_{\perp p}/T_{\| p}$) and the electron temperature anisotropy are important and major factors.

3.1. Magnetosheath Plasma: Isotropic Electrons

[11] The solar wind plasma is observed to contain traces of ions of helium, oxygen, etc. So it is realistic to assume that the magnetosheath plasma is more than just a two-component electron-proton plasma. In this section, we consider a four-component plasma with electrons, protons, and two minor ions: helium ($^4He^{2+}$) and oxygen ($^{16}O^{6+}$). Our purpose is to demonstrate how the presence of these heavy ions alter the β_p and $T_{\perp p}/T_{\| p}$ threshold for mirror dominance. Here we deal with isotropic electrons but all other species will have equal temperatures and anisotropies as that of the protons.

[12] Table 1 illustrates the growth rates of the ion cyclotron and mirror instabilities at two different (β_p, $T_{\perp p}/T_{\| p}$) values, one with $\beta_p < 1.0$ and the other with $\beta_p > 1.0$, for three different helium concentrations $n_\alpha = 0.01 n_p$, $n_\alpha = 0.04 n_p$, and $n_\alpha = 0.10 n_p$. The (β_p, $T_{\perp p}/T_{\| p}$) values (0.5, 2.5) and (4.0, 1.4) are chosen such that for the low beta value $\beta_p = 0.5$, it follows from the instability condition given by [*Chandrasekhar et al*., 1958] that the temperature anisotropy should be high enough to excite the mirror waves, and for a high beta value of $\beta_p = 4.0$, the effect of the heavy ions is found significant for low anisotropy values (close to threshold). From Table 1, it is clear that for the (β_p, $T_{\perp p}/T_{\| p}$) value (4.0, 1.4), the mirror growth exceeds the ion cyclotron growth rate at $n_\alpha = 0.04 n_p$, whereas when the heavy ion concentration is increased to $n_\alpha = 0.10 n_p$, the mirror growth rate is greater than the corresponding ion cyclotron growth rate at much lower beta $\beta_p = 0.5$. This indicates that higher concentrations of heavy ions favor the mirror wave dominance at much lower beta value ($\beta_p = 0.5$). In the absence of heavy ions, the mirror instability was found to be dominating for plasma betas greater than 10.0. Such high betas are not expected downstream of quasi-perpendicular shocks. Thus, these cases are extreme and are not expected in planetary magnetosheaths.

[13] Figure 1 represents the growth rate curves of the ion cyclotron instability (top) and mirror instability (bottom) for three different helium concentrations $n_\alpha = 0.01 n_p$ (plus sign), $n_\alpha = 0.04 n_p$ (asterisk), and $n_\alpha = 0.10 n_p$ (circle). We can see that the presence of the minor ions reduces the growth rate of the ion cyclotron instability significantly whereas it slightly increases the growth rate of mirror instability [*Price et al*., 1986].

[14] Figure 2 shows the maximum growth rate γ_m (maximized with respect to the normalized wave number $K = k v_{thp}/\Omega_p$) dependence on heavy ion density for the $T_{\perp p}/T_{\| p} = 1.4$ case. The mirror instability is shown in triangles and the ion cyclotron instability in asterisks. It can be noted that for heavy ion fractional densities, N_m/n_p greater than 0.03, the mirror will dominate. Here $N_m = n_\alpha + n_O$ and the contribution of O^{6+} ion is negligible unless we consider it to be present in very high concentrations.

[15] Figure 3 shows the variation in the maximum growth rates of the ion cyclotron (solid line) and mirror (dashed line) modes with respect to the proton temperature anisotropy in $\beta_p = 4.0$ plasma. It can be seen that there is a transition of the mirror dominant plasma to ion cyclotron-dominant plasma. We observed that above an anisotropy value 1.43, the ion cyclotron growth rates exceeds the mirror growth; that is, the mirror dominance is only at or below the anisotropy value 1.43 for $\beta_p = 4.0$ plasma, or the effect of the

Table 1. Growth Rates: Isotropic Electrons

(β_p, $T_{\perp p}/T_{\| p}$)	$\gamma_m/\Omega_p(ICI^*)$			$\gamma_m/\Omega_p(MI^*)$		
	$n_\alpha = 0.01 n_p$	$n_\alpha = 0.04 n_p$	$n_\alpha = 0.10 n_p$	$n_\alpha = 0.01 n_p$	$n_\alpha = 0.04 n_p$	$n_\alpha = 0.10 n_p$
(0.5, 2.5)	0.0513	0.0257	0.0069	0.0072	0.0079	0.0093
(4.0, 1.4)	0.0115	0.0078	0.0056	0.0084	0.0088	0.0095

*ICI indicates ion cyclotron instability and MI refers to mirror instability.

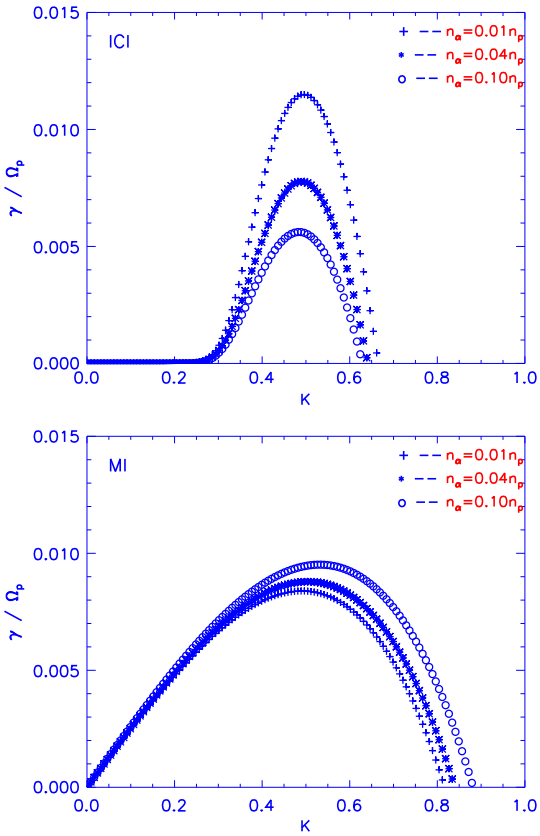

Figure 1. Growth rate of proton cyclotron anisotropy instability (top) and mirror instability (bottom) as functions of normalized wave number ($K=kv_{thp}/\Omega_p$) for $\beta_p=4.0$ for $n_\alpha=0.01n_p$ (plus sign), $n_\alpha=0.04n_p$ (asterisk), and $n_\alpha=0.10$ n_p (circle) at $T_{\perp p}/T_{\| p}=1.4$. ICI indicates ion cyclotron instability and MI refers to mirror instability.

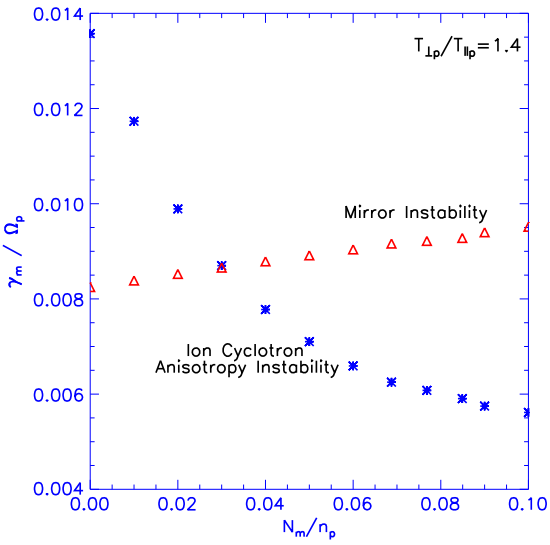

Figure 2. The maximum growth rate of the ion cyclotron (asterisks) and mirror (triangle) instabilities as functions of relative minor ion density N_m/n_p ($N_m=n_\alpha+n_O$) at $\beta_p=4.0$, $T_{\perp\alpha}/T_{\|\alpha}=T_{\perp O}/T_{\| O}=T_{\perp p}/T_{\| p}=1.4$.

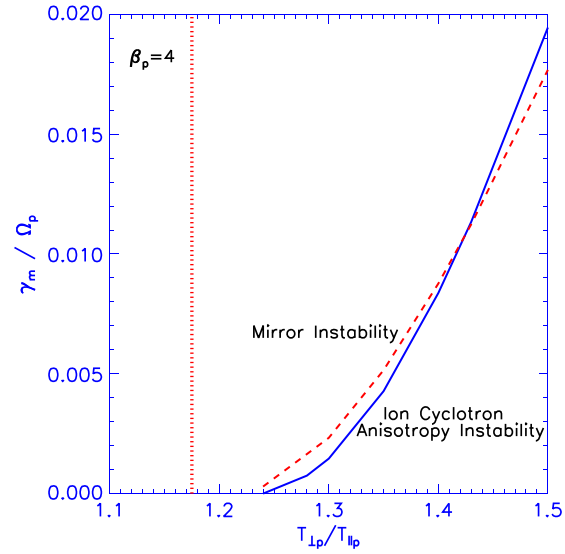

Figure 3. The maximum growth rate curves of ion cyclotron (solid line) and mirror (dashed line) instabilities as functions of proton anisotropy in a multi-species plasma at $\beta_p=4.0$. The transition between the mirror dominant regime to ion cyclotron dominance is seen to occur at $T_{\perp p}/T_{\| p}\simeq 1.43$. Here $n_\alpha=0.04n_p$, $n_O=0.04n_\alpha$, $T_{\perp\alpha}/T_{\|\alpha}=T_{\perp O}/T_{\| O}=T_{\perp p}/T_{\| p}$, $T_{\perp e}=T_{\| e}$, and $T_{\|\alpha}=T_{\| O}=T_{\| e}=T_{\| p}$. The dotted line indicates the proton anisotropy threshold value ($T_{\perp p}/T_{\| p}=1.175$).

presence of minor ions is significant only when the anisotropy is near the threshold value (1.18 in this case) [*Gary*, 1992].

[16] Figures 4 and 5 depict the effect of the temperature and anisotropy of the heavy ions on the ion cyclotron and mirror mode frequencies, respectively. The solid lines are the real frequencies and the dashed lines are for the growth rates. The concentration, temperature, and the anisotropy of the heavy ions do not significantly alter the real frequency but alter the growth rates of both the instabilities. As the temperature and anisotropy of the minor ions are increased, the growth rates of both instabilities show a rise.

3.2. Magnetosheath Plasma: Anisotropic Electrons

[17] In this section we incorporate the effect of anisotropic electrons in a multi-component plasma model and show how the electron anisotropy becomes a significant factor in determining the competition between the mirror and ion cyclotron instabilities. Here we consider electrons and all the ions to have equal temperature and anisotropy as that of the protons. Since electrons may reach an isotropic distribution faster, as compared to protons, the anisotropy of electrons is considered to be smaller than that of the protons.

[18] Figure 6 illustrates how the growth rates of the ion cyclotron (top) instability vary as a function of wave number with the introduction of electron anisotropy ($n_\alpha=0.01n_p$ case). Here we take the case of a very small electron anisotropy, $T_{\perp e}/T_{\| e}=1.2$. The dispersion relation for the electromagnetic ion cyclotron mode for our bi-Maxwellian plasma model can be written as [*Stix*, 1962; *Montgomery*

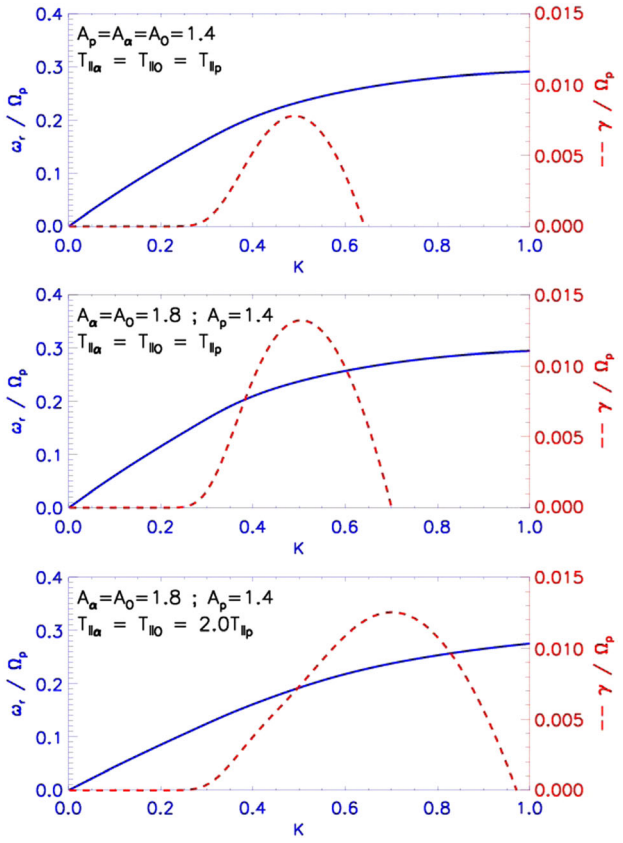

Figure 4. The real (solid lines) and imaginary (dashed lines) frequency of the ion cyclotron anisotropy instability as functions of normalized wave number for $\beta_p = 4.0$ and proton anisotropy 1.4. The first panel corresponds to $A_\alpha = A_O = A_p = 1.4$ and $T_{\|\alpha} = T_{\|O} = T_{\|p}$; the second panel indicates $A_\alpha = A_O = 1.8$, $A_p = 1.4$, and $T_{\|\alpha} = T_{\|O} = T_{\|p}$; and the third panel shows $A_\alpha = A_O = 1.8$, $A_p = 1.4$, and $T_{\|\alpha} = T_{\|O} = 2T_{\|p}$. Here $n_\alpha = 0.04 n_p$.

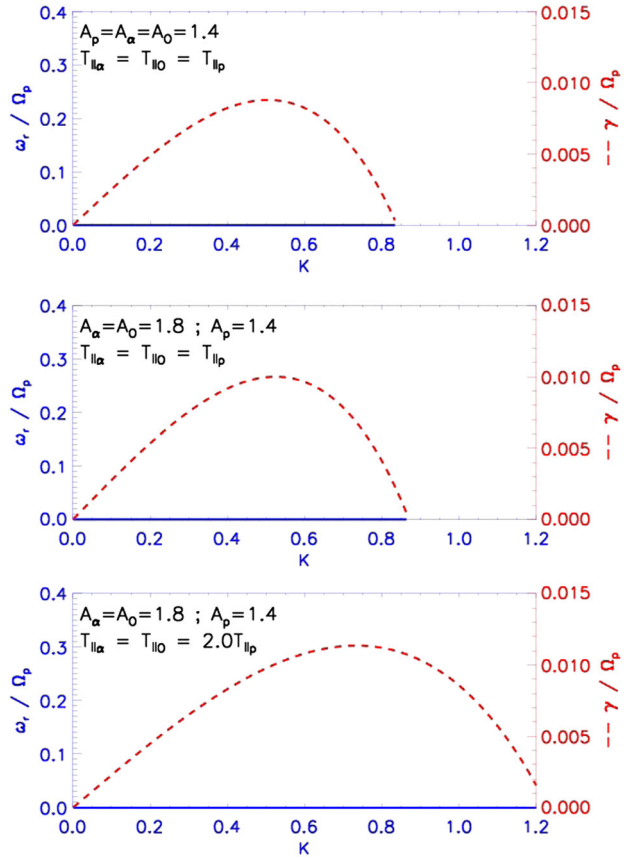

Figure 5. The real (solid lines) and imaginary (dashed lines) frequency of the mirror instability as functions of normalized wave number for $\beta_p = 4.0$ and proton anisotropy 1.4. The first panel corresponds to $A_\alpha = A_O = A_p = 1.4$ and $T_{\|\alpha} = T_{\|O} = T_{\|p}$; the second panel indicates $A_\alpha = A_O = 1.8$, $A_p = 1.4$, and $T_{\|\alpha} = T_{\|O} = T_{\|p}$; and the third panel shows $A_\alpha = A_O = 1.8$, $A_p = 1.4$, and $T_{\|\alpha} = T_{\|O} = 2T_{\|p}$. Here $n_\alpha = 0.04 n_p$.

and Tidman, 1964; *Scharer and Trivelpiece*, 1967; *Lakhina and Buti*, 1976]

$$\frac{c^2k^2}{\omega^2} = 1 + \sum_j \frac{\omega_j^2}{\omega^2}\left\{A_j - 1 + Z\left(\eta_j\right)\left[\frac{\Omega_j}{kv_{thj}} + A_j\eta_j\right]\right\} \qquad (2)$$

where $\omega_j^2 = \frac{4\pi n_j q_j^2}{m_j}$ is the plasma frequency of the species j, $Z(\eta_j)$ is the plasma dispersion function [*Fried and Conte*, 1961], and the resonance parameter $\eta_j = \frac{\omega - \Omega_j}{kv_{thj}}$. It is clear that the growth rate of the proton cyclotron instability is directly related to the resonance term η_j. The proton resonance parameter η_p is also shown on the plot (top). It can be seen that the introduction of an electron anisotropy decreases the growth rate and the unstable wave number range for the ion cyclotron modes, whereas it does not significantly affect η_p. This shows that the reduction of the growth rate by anisotropic electrons is not due to changes in the proton resonance term, or in other words the proton resonance is unaltered by the presence of anisotropy in electrons. It appears that in the presence of anisotropic electrons, the growth rate of the ion cyclotron instability is reduced by the increase of proton threshold anisotropy and the reduction in the upper limit on unstable wave numbers. It can be seen from Figure 6 (top) that the upper limit of the unstable wave numbers reduced from 0.66 to 0.55, approximately, which means that the electron temperature anisotropy has restrained the growth of ion cyclotron instability to longer wavelengths. Figure 6 (bottom) plots the growth rates of the mirror modes with and without the inclusion of electron anisotropy (dashed and solid curves, respectively). Here the growth rate has increased about five times and the range of unstable wave number has doubled as we included the electron anisotropy. It indicates that the mirror instability grows for a wider wave vector space in the presence of electron temperature anisotropy.

[19] Table 2 summarizes the growth rates of the ion cyclotron and mirror instabilities for two different electron anisotropies in $\beta_p = 0.5$ plasma. Here we can see that an increase in electron anisotropy from $T_{\perp e}/T_{\|e} = 1.2$ to $T_{\perp e}/T_{\|e} = 1.8$ has further reduced the ion cyclotron growth and enhanced the mirror mode growth rate. This makes the mirror mode dominant in plasmas with $\beta_p = 0.5$ even with heavy ion concentration as low as $n_\alpha = 0.01 n_p$. It indicates that the electron temperature anisotropy is a major cause for the mirror dominance in low beta plasmas. The effect of electron

temperature anisotropy on the growth rates is found to be valid even in the absence of heavy ions. So if we consider that the magnetosheath plasma consists of electrons having temperature anisotropy equal to or less than that of the protons, then the mirror modes can easily predominate in this region even without the inclusion of heavy ions.

[20] Figure 7 illustrates the variation of the maximum growth rate of the ion cyclotron (solid line) and mirror (dashed line) instability as a function of increasing electron temperature anisotropy. It is clear that as electron temperature anisotropy is increased, the maximum growth rate of the ion cyclotron instability keeps on decreasing monotonically, but that of mirror modes goes on increasing. Therefore, the higher the electron temperature anisotropy, the higher is the probability that the mirror modes will outgrow the ion cyclotron modes.

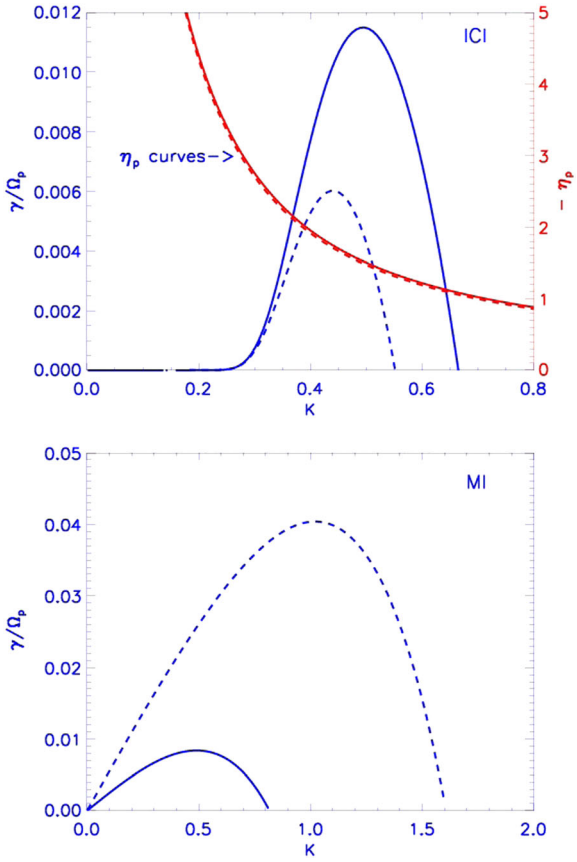

Figure 6. The growth rates γ/Ω_p of the ion cyclotron instability (top) for isotropic (solid curve) and anisotropic electrons (dashed curve) as a function of normalized wave number in the presence of heavy ions ($n_\alpha = 0.01 n_p$) at $\beta_p = 4.0$ and $T_{\perp p}/T_{\| p} = 1.4$. The corresponding proton resonance term η_p is plotted in the right-hand side y axis. The bottom panel gives the corresponding growth rates for the mirror instability. Temperature anisotropy of electrons considered here is $T_{\perp e}/T_{\| e} = 1.2$.

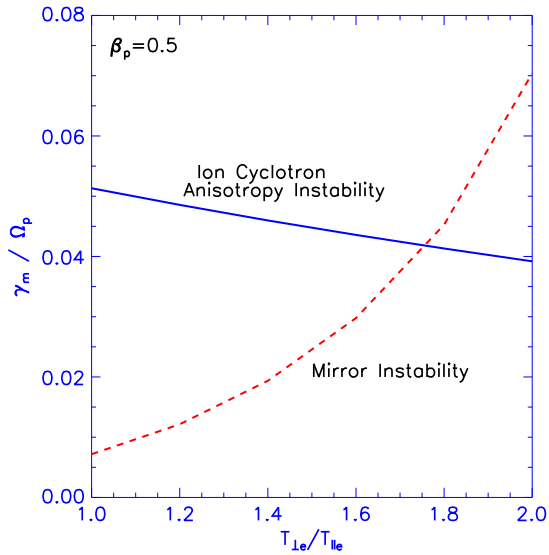

Figure 7. Maximum growth rate as a function of $T_{\perp e}/T_{\| e}$ for proton cyclotron (solid line) and mirror (dashed line) instabilities in a $\beta_p = 0.5$ plasma. Here $n_\alpha = 0.01 n_p$.

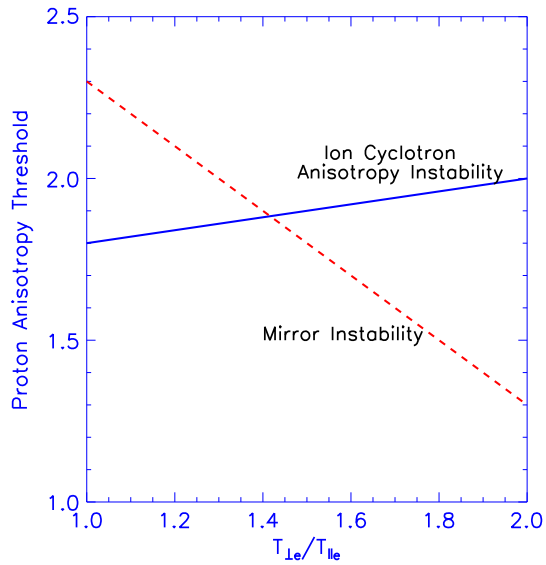

Figure 8. Proton anisotropy threshold as a function of $T_{\perp e}/T_{\| e}$ for ion cyclotron (solid line) and mirror (dashed line) instabilities in a $\beta_p = 0.5$ plasma.

Table 2. Growth Rates: Anisotropic Electrons ($\beta_p = 0.5$, $T_{\perp p}/T_{\| p} = 2.5$)

$T_{\perp e}/T_{\| e}$	γ_m/Ω_p (ICI*)			γ_m/Ω_p (MI*)		
	$n_\alpha = 0.01 n_p$	$n_\alpha = 0.04 n_p$	$n_\alpha = 0.10 n_p$	$n_\alpha = 0.01 n_p$	$n_\alpha = 0.04 n_p$	$n_\alpha = 0.10 n_p$
1.2	0.0486	0.0221	0.0006	0.0122	0.0132	0.0150
1.8	0.0413	0.0125	0.0004	0.0453	0.0489	0.0564

*ICI indicates ion cyclotron instability and MI refers to mirror instability.

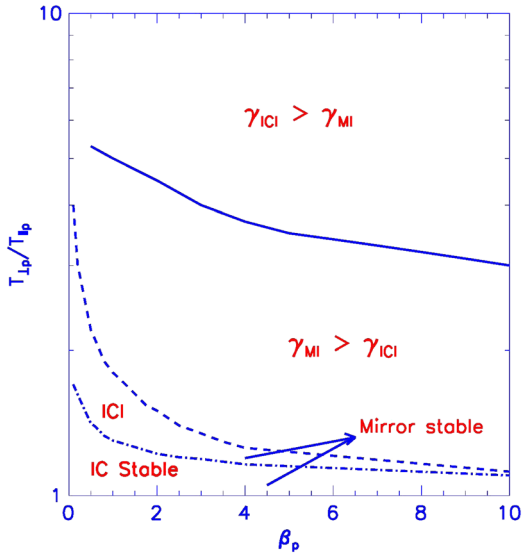

Figure 9. The existence regimes for the mirror and ion cyclotron anisotropy instability in a ($\beta_p - T_{\perp p}/T_{\parallel p}$) plane. γ_{ICI} and γ_{MI} indicate growth rates of ion cyclotron and mirror instability, respectively. ICI indicates ion cyclotron instability and MI refers to mirror instability. Electron temperature anisotropy for this case is $T_{\perp e}/T_{\parallel e} = 1.2$.

[21] Figure 8 shows the proton anisotropy threshold for the ion cyclotron instability and mirror instability as a function of $T_{\perp e}/T_{\parallel e}$. The ion cyclotron instability is shown as solid line and the mirror instability as dashed line. The figure indicates that the inclusion of electron temperature anisotropy increases the proton anisotropy threshold for the ion cyclotron instability which means that its growth rate will be reduced, whereas proton anisotropy threshold decreases for the mirror modes indicating an increase in the corresponding growth rates.

[22] Figure 9 shows the ($\beta_p, T_{\perp p}/T_{\parallel p}$) parameter regions for the existence of the mirror and ion cyclotron modes. The region of very low beta and low proton temperature anisotropy (below the dashed-dotted line) shows the region where both the ion cyclotron and mirror modes are stable. The region above this line and below the dashed line indicates a mirror stable region where we can expect only the ion cyclotron instability to grow. Above this line, both the mirror and ion cyclotron modes are unstable and whichever has a higher growth rate prevails. The boundary marked here (solid line) portrays an approximate demarcation for the regions where each of the mirror and ion cyclotron modes dominate for a constant electron temperature anisotropy. Variation in electron temperature anisotropy will result in variation of the curve boundaries.

4. Summary

[23] To summarize,

[24] 1. Linear theory results to date clearly indicate that the proton cyclotron anisotropy instability grows faster than mirror modes for a wide parametric regime in an electron-proton plasma containing isotropic electrons and anisotropic protons. The mirror instability dominates for plasma beta > 10.0. Such large values of betas are unrealistic for planetary magnetosheaths and hence the results are not shown.

[25] 2. The inclusion of anisotropic heavy ions $^4He^{2+}$ and $^{16}O^{6+}$ in the magnetosheath plasma model with isotropic electrons showed substantial reduction in the ion cyclotron growth rate while leaving the mirror mode growths essentially unaltered. This results in higher mirror mode growth rates at lower beta values of about $\beta_p = 4.0$ for helium concentration of $n_\alpha = 0.04 n_p$. The beta value can still be reduced to $\beta_p = 0.5$ if the helium density is considered to be higher ($n_\alpha = 0.10 n_p$). The contribution of $^{16}O^{6+}$ ion was found to be negligible compared to the $^4He^{2+}$ contribution. An increase in anisotropy and temperature of the heavy ions increases the growth rates of both the mirror and ion cyclotron instabilities.

[26] 3. The inclusion of electron temperature anisotropies in the plasma model further suppresses the growth rate of the ion cyclotron modes and enhances the mirror mode growths for a wide range of plasma betas. For $T_{\perp e}/T_{\parallel e} = 1.2$ mirror mode growth exceeds the ion cyclotron growth at a beta value $\beta_p = 0.5$ with a helium concentration $n_\alpha = 0.10 n_p$. Increasing the electron anisotropy to $T_{\perp e}/T_{\parallel e} = 1.8$, the mirror modes dominate at $\beta_p = 0.5$ for $n_\alpha = 0.01 n_p$ (Figure 7). The presence of electron anisotropy could possibly explain the mirror structures found in low beta magnetopause regions [*Tátrallyay and Erdos*, 2005].

[27] 4. Based on the detailed parametric analysis, we obtained a general picture of the parametric regimes over which each of these instabilities exists. With a small amount of heavy ions like helium (~1% to 10% of proton density) and oxygen (~4% of helium density), and an electron temperature anisotropy ($\sim T_{\perp e}/T_{\parallel e} = 1.2$), mirror modes dominate in a wide parameter space. Below certain critical values (very low beta and low temperature anisotropies), mirror modes were found to be stable.

5. Discussion and Conclusions

[28] The linear kinetic dispersion relation is solved numerically using the WHAMP code to study the growth rates and dispersion properties of the two major low frequency temperature anisotropy instabilities, mirror and ion cyclotron anisotropy instability, in planetary magnetosheath regions.

[29] Our numerical results of linear Vlasov theory show that inclusion of anisotropic heavy ions like He^{2+} and O^{6+} in small quantity to the magnetosheath plasma model sufficiently reduced the ion cyclotron growth rate while slightly increasing the mirror growth. The additional heavy ions resonate with the proton cyclotron instability at their gyrofrequencies due to which the ion cyclotron mode propagation is possible for a band of frequencies whose upper limits are the gyrofrequencies of each ion [*Gintsburg*, 1963]. The resonances (frequencies at which refractive index is infinite) and the cutoffs (frequencies at which refractive index is zero) for ion cyclotron propagation in a multicomponent plasma have been derived and well explained [*Stix*, 1962; *Smith and Brice*, 1964; *Gintsburg*, 1965; *Horne and Thorne*, 1993]. Several ion cyclotron waves at different frequencies will thus create stop bands which in turn will cut the linear growth rate of the proton cyclotron instability

whereas the additional free energy enhances the non-resonant mirror mode growth. The helium ion concentration was varied between 1% and about 10% of the proton density in order to model all the possible magnetosheath configurations and O^{6+} density was assumed to be about 4% of the helium density. The mirror mode growth rates were found to be greater than the ion cyclotron growth at $\beta_p = 4.0$ when the heavy ion concentration was $n_\alpha = 0.04 n_p$. This is possible only at anisotropy values close to threshold. The explanation for this is rather simple. We know that mirror modes have a higher anisotropy threshold compared to the ion cyclotron modes. So at high beta values, when the temperature anisotropy is close to threshold, the growth rate of the ion cyclotron mode will be marginal and hence the comparatively low frequency mirror mode gets excited. For anisotropy values away from threshold, the usual scenario persists. Many of the Earth's magnetosheath observations indicate that the plasma beta in the deep magnetosheath is typically high ($\beta_p \gg 1$) with sufficiently low temperature anisotropies [*Fuselier et al*., 1991; *Soucek and Escoubet*, 2011; *Tátrallyay and Erdos*, 2005]. Our studies here confirm that it is not unusual to find mirror mode waves excited in such regions. If the He^{2+} density is increased to about 10% of proton density then the mirror mode prevails even in $\beta_p = 0.5$ plasma away from threshold anisotropies.

[30] Introducing an electron temperature anisotropy further lowers the beta threshold for the mirror mode dominance even in the absence of heavy ions. For an electron anisotropy $T_{\perp e}/T_{\| e} = 1.8$, mirror modes were found to be prevalent in $\beta_p = 0.5$ plasma with $n_\alpha = 0.01 n_p$. The electron temperature anisotropy suppresses the growth rate of ion anisotropy instability by increasing the proton anisotropy threshold and reducing the upper limit on unstable wave numbers. It was also found that the electron anisotropy does not alter the ion cyclotron resonance. At the same time, additional energy in the electron anisotropy enhances the growth rate of mirror instability and increases the upper limit on unstable wave numbers for a wide range of plasma betas. As a consequence, the mirror waves can surmount the electromagnetic ion anisotropy instability in plasmas even with low beta conditions. Including heavy ions in the plasma model enhances the effect. The evolution of mirror instability waves in the low beta regions can hence be explained on two grounds: electron temperature anisotropy and high heavy ion concentrations ($\sim n_\alpha = 0.10 n_p$). Higher values of electron anisotropies ($T_{\perp e}/T_{\| e} \geq 1.8$) yield prevalent mirror mode structures in $\beta_p < 0.5$ plasmas. The faster isotropization of electrons restricts us to have electron anisotropies lesser than that of protons and other ions. To our knowledge, this is the first study to incorporate the effect of electron temperature anisotropies to analyze the competition between the two major low frequency ion modes, mirror and ion cyclotron anisotropy instabilities, in the planetary magnetosheaths.

[31] The results of our study based on the linear growth rates are valid in the small amplitude limit. Mirror instability is found to grow to very high amplitudes of the order of $\delta B \sim B_0$ to nonlinear limits. Thus, the nonlinear studies are very important to understand the wave-particle interactions which could lead to further growth/damping of these wave modes. The simulations in two or three dimensions will be appropriate to infer the physics behind the two competing instabilities.

[32] The competition between the mirror instability and the ion cyclotron instability is particularly interesting at and near the termination shock. Because of the Parker spiral magnetic field windup, it is expected that the termination shock will typically be a perpendicular one at these large distances. Both ion and electron heating in perpendicular temperature will occur. It is thus expected that the mirror instability will dominate immediately downstream of the shock. However further downstream, electron instabilities may be quenched with the isotropization of electrons. Then the ion cyclotron instabilities may dominate. Observations will be able to tell whether this scenario is a correct one or not.

[33] **Acknowledgments.** G.S.L. thanks the Indian National Science Academy, New Delhi, for the support under the Senior Scientist Scheme. Portions of this research were performed at the Jet Propulsion Laboratory, California Institute of Technology under contract with NASA. Thanks are due to Fundacao de Amparo a Pesquisa do Estado de Sao Paulo (FAPESP, Project 2012/05397-3) for the fellowship to G.S.L. to visit Instituto Nacional de Pesquisas Espaciais (INPE), Sao Jose dos Campos, Brazil. B. Remya would like to thank the Indian Institute of Geomagnetism, Navi Mumbai, India, for providing her with a Senior Research Fellowship to carry out this research work. E.E. acknowledges CNPQ agency contract 301233/2011-0 and FAPESP agency contract 2012/06673-4 for support in this work.

References

Anderson, B. J., S. A. Fuselier, and D. Murr (1991), Electromagnetic ion cyclotron waves observed in the plasma depletion layer, *Geophys. Res. Lett.*, *18*, 1955–1958.

Anderson, B. J., and S. A. Fuselier (1993), Magnetic pulsations from 0.1 to 4.0 Hz and associated plasma properties in the Earth's subsolar magnetosheath and plasma depletion layer, *J. Geophy. Res.*, *98*, 1461–1479.

Bame, S. J., A. J. Hundhausen, J. R. Asbridge, and I. B. Strong (1968), Solar wind ion composition, *Phys. Rev. Lett.*, *20*, 393.

Bame, S. J., J. R. Asbridge, A. J. Hundhausen, and M. D. Montgomery (1970), Solar wind ions: $^{56}Fe^{+8}$ to $^{56}Fe^{+12}$, $^{28}Si^{+7}$, $^{28}Si^{+8}$, $^{28}Si^{+9}$, and $^{16}O^{+6}$, *J. Geophy. Res.*, *75*, 6360–6365.

Barnes, A. (1966),Collisionless damping of hydromagnetic waves, *Phys. Fluids*, *9*, *1483*.

Burlaga, L. F., N. F. Ness, and M. H Acuna (2006), Trains of magnetic holes and magnetic humps in the heliosheath, *Geophy. Res. Lett.*, *33*, L21106.

Burlaga, L. F., N. F. Ness, and M. H. Acuna (2007), Linear magnetic holes in a unipolar region of the heliosheath observed by Voyager 1, *J. Geophys. Res.*, *112*, A07106, doi:10.1029/2007JA012292.

Chandrasekhar, S., A.N. Kaufman, and K. M. Watson (1958), The stability of the pinch, *Proc. R. Soc. London, Ser. A*, *245*, 435–455.

Erdös, G, and A Balogh (1996), Statistical properties of mirror mode structures observed by Ulysses in the magnetosheath of Jupiter, *J. Geophy. Res*, *101* (A1), 1–12.

Fried, B. D, and S. D Conte (1961), The plasma dispersion function, Academic, San Diego, California.

Fuselier, S. A., D. M. Klumpar, E. G. Shelly, B. J. Anderson, and A. J. Coates (1991), He^{2+} and H^+ dynamics in the subsolar magnetosheath and plasma depletion layer, *J. Geophy. Res.*, *96*, 21095.

Gary, S. P., M. D.Montgomery, W. C. Feldman, and D. W. Forslund (1976), Proton temperature anisotropy instabilities in the solar wind, *J. Geophy. Res.*, *81*, 1241.

Gary, S. P. (1992), The mirror and ion cyclotron anisotropy instabilities, *J. Geophy. Res.*, *97*, 8519.

Gary, S. P, S. A Fuselier, and B. J Anderson (1993), Ion anisotropy instabilities in the magnetosheath, *J. Geophy. Res.*, *98*, 1481–1488.

Gary, S. P., M. E. McKean, and D. Winske (1993), Ion cyclotron anisotropy instabilities in the magnetosheath: Theory and simulations, *J. Geophy. Res.*, *98*, 3963–3971.

Gintsburg, M. A. (1963), Low-frequency waves in multicomponent plasma, *Geomagnetism Aeronomy*, *3*, 610–614.

Gintsburg, M. A. (1965), Ion cyclotron whistlers, *J. Geophy. Res.*, *70*, 1665.

Hasegawa, A. (1969), Drift mirror instability in the magnetosphere, *Phys. Fluids*, *12*, 2642–2650, doi:10.1063/1.1692407.

Horne, R. B., and R. M. Thorne (1993), On the preferred source location for the convective amplification of ion cyclotron waves, *J. Geophy. Res.*, *98*, 9233–9247, doi:10.1029/92JA02972.

Kaufmann, R. L., J.-T. Horng, and A. Wolfe (1970), Large-amplitude hydromagnetic waves in the inner magnetosheath, *J. Geophy. Res.*, *75*, 4666.

Kennel, C. F., and H. E. Petschek (1966), Limit on stably trapped particle fluxes, *J. Geophy. Res.*, *71*, 1.

Lucek, E. A., M. W. Dunlop, T. S. Horbury, A. Balogh, P. Brown, P. Cargill, C. Carr, K.-H. Fornacon, E. Georgescu, and T. Oddy (2001), Cluster magnetic field observations in the magnetosheath: Four-point measurements of mirror structures, *Ann. Geophys.*, *19*, 1421–1428, doi:10.5194/angeo-19-1421-2001.

Lacombe, C., F. G. E. Pantellini, D. Hubert, C. C. Harvey, A. Mangeney, G. Belmont, and C. T. Russell (1992), Mirror and Alfvenic waves observed by ISEE 1–2 during crossings of the Earth's bow shock, *Ann. Geophys.*, *10*, 772.

Lakhina, G. S., and B. Buti (1976), Stability of solar wind double ion streams, *J. Geophy. Res.*, *81*, 2135.

Lee, L.-C., C. S. Wu, and C. P. Price (1987), On the generation of magnetosheath lion roars, *J. Geophy. Res.*, *92*, 2343–2348.

Lee, L.-C., C. P. Price, C. S. Wu, and M. E. Mandt (1988), A study of mirror waves generated downstream of a quasi-perpendicular shock, *J. Geophy. Res.*, *93*, 247–250.

Masood, W., and S. J. Schwartz (2008), Observations of the development of electron temperature anisotropies in Earth's magnetosheath, *J. Geophy. Res.*, *113*, 12.

Midgley, J. E., and L. Davis Jr (1963), Calculation by a moment technique of the perturbation of the geomagnetic field by the solar wind, *J. Geophy. Res.*, *68*, 5111.

Montgomery, D.C., and D. A. Tidman (1964), *Plasma Kinetic Theory*, McGraw-Hill, New York.

Price, C. P., D. W. Swift, and L.-C. Lee (1986), Numerical simulation of nonoscillatory mirror waves at the Earth's magnetosheath, *J. Geophy. Res.*, *91*, 101.

Ronnmark, K. (1982), WHAMP—Waves in homogeneous anisotropic multicomponent plasma, Kiruna Geophysical Institute Report, 179.

Ronnmark, K. (1983), Computation of the dielectric tensor of a Maxwellian plasma, *Plasma Phy.*, *25*, 699.

Russell, C.T., W. Riedler, K. Schwingenschuh, and Y. Yeroshenko (1987), Mirror instability in the magnetosphere of Comet Halley, *Geophy. Res. Lett.*, *14*, 644–647.

Scharer, J. E., and A. W. Trivelpiece (1967), Cyclotron instabilities in plasma, *Phys. Fluids*, *10*, 591.

Schwartz, S. J., D. Burgess, and J. J. Moses (1996), Low-frequency waves in the Earth's magnetosheath: Present status, *Ann. Geophys.*, *14*, 1134–1150.

Sckopke, N., G. Paschmann, A. L. Brinca, C. W. Carlson, and H. Lühr (1990), Ion thermalization in quasi-perpendicular shocks involving reflected ions (1990), *J. Geophy. Res.*, *95*, 6337–6352.

Shoji, M., Y. Omura, B. T. Tsurutani, O. P. Verkhoglyadova, and B. Lembege (2009), Mirror instability and L-mode electromagnetic ion cyclotron instability: Competition in the Earth's magnetosheath, *J. Geophy. Res.*, *114*, A10203, doi:10.1029/2008JA014038.

Shoji, M., Y. Omura, L. Lee (2012), Multidimensional nonlinear mirror-mode structures in the Earth's magnetosheath, *J. Geophy. Res.*, *117*, A08208, doi:10.1029/2011JA017420.

Smith, R. L., and N. Brice, Propagation in multicomponent plasmas (1964), *J. Geophys. Res.*, *69*, 5029–5040.

Song, P., C. T. Russell, and M. F. Thomsen (1992), Waves in the inner magnetosheath: A case study, *Geophy. Res. Lett.*, *19*, 2191.

Soucek, J., and C. P. Escoubet (2011), Cluster observations of trapped ions interacting with magnetosheath mirror modes, *Ann. Geophys.*, *29*, 1049–1060.

Stix, T. H. (1962), The Theory of Plasma Waves, McGraw-Hill, New York.

Tátrallyay, M., and G. Erdos (2005), Statistical investigation of mirror type magnetic field depressions observed by ISEE-1, *Planet. Space Sci.*, *50*, 593–599.

Thomsen, M. F., J. T. Goslling, S. J. Bame, and M. M. Mellott (1985), Ion and electron heating at collisionless shocks near the critical Mach number, J. Geophy. Res, *90*, 137.

Tsurutani, B. T, E. J Smith, R. R Anderson, K. W Ogilvie, J. D Scudder, D. N Baker, and S. J Bame (1982), Lion roars and nonoscillatory drift mirror waves in the magnetosheath, *J. Geophy. Res*, *87*, 6060–6072.

Tsurutani, B. T, I. G Richardson, R. P Lepping, R. D Zwickl, D. E Jones, E. J Smith, and S. J Bame (1984), Drift mirror waves in the distant (X ≅200 Re) magnetosheath, *Geophys. Res. Lett.*, *11*, 1102–1105, doi:10.1029/GL011i010p01102.

Tsurutani, B. T, D. J Southwood, E. J Smith and A Balogh (1992), Nonlinear magnetosonic waves and mirror modes structures in the March 1991 ULYSSES interplanetary event, *Geophy. Res. Lett*, *19*, 1267–1270.

Tsurutani, B. T, G. S Lakhina, E. J. Smith, B. Buti, S. L. Moses, F. V. Coroniti, A. L. Brinca, J. A. Slavin, and R. D. Zwickl (1999), Mirror mode structures and ELF plasma waves in the Giacobini-Zinner magnetosheath, *Nonlinear Process. Geophys.*, *6*, 229–234, doi:10.5194/npg-6-229–1999.

Tsurutani, B. T., J. K. Arballo, X.-Y. Zhou, C. Galvan, and J. K. Chao (2000), Electromagnetic electron and proton cyclotron waves in geospace: A Cassini snapshot, space weather study using multipoint techniques, Proceedings of the COSPAR Colloquium held in Pacific Green Bay, Taiwan, September, 2000, edited by Ling-Hsiao Lyu., Pergamon Press. p 97

Tsurutani, B. T., E. Echer, O. P. Verkhoglyadova, G. S. Lakhina, and F. L. Guarnieri (2010), Mirror instability upstream of the termination shock(TS) and in the heliosheath, *J. Atmos. Sol. Terr. Phys.*, *73*, 1398–1404.

Tsurutani, B. T., G. S. Lakhina, O. P. Verkhoglyadova, E. Echer, F. L. Guarnieri, Y. Narita, and D. O. Constantinescu (2011), Magnetosheath and heliosheath mirror mode structures, interplanetary magnetic decreases, and linear magnetic decreases: Differences and distinguishing features, *J. Geophy. Res.*, *116*, A02103, doi:10.1029/2010JA015913.

Vedenov, A. A., and R. Z. Sagdeev (1958), Some properties of a plasma with an anisotropic ion velocity distribution in a magnetic field, in *Plasma Physics and the Problem of Controlled Thermonuclear Reactions, Vol.3*, pp.332–339, Pergamon, New York.

Winske, D., and K. B. Quest (1988), Magnetic field and density fluctuations at perpendicular supercritical collisionless shocks, *J. Geophy. Res.*, *93*, 9681–9693.

Zwan, B. J., and R. A. Wolf (1976), Depletion of the solar wind plasma near a planetary boundary, *J. Geophy. Res.*, *81*, 1636–1648, doi:10.1029/JA081i010p01636.